Physics of the Earth and Planetary Interiors 189 (2011) 117–120

Contents lists available at ScienceDirect

Physics of the Earth and Planetary Interiors

journal homepage: www.elsevier.com/locate/pepi

Short communication

Prospecting for water in the transition zone: $d\ln(Vs)/d\ln(Vp)$

Li Li [a,*], Donald J. Weidner [a], John P. Brodholt [b], Dario Alfè [b]

[a] *Mineral Physics Institute, Department of Geosciences, University of New York at Stony Brook, Stony Brook, NY 11790, USA*
[b] *Department of Earth Sciences, University College London, Gower Street, London WC1E6BT, UK*

ARTICLE INFO

Article history:
Received 11 April 2011
Received in revised form 9 July 2011
Accepted 13 July 2011
Available online 16 August 2011
Edited by Mark Jellinek

Keywords:
$d\ln(Vs)/d\ln(Vp)$
Water
Transition zone
Mantle
Lateral heterogeneity

ABSTRACT

We report the values of $R = d\ln(Vs)/d\ln(Vp)$ due to water as a function of pressure for Mg_2SiO_4 olivine, wadsleyite, ringwoodite. The results show that ringwoodite has significantly lower *R* than olivine and wadsleyite; due to the reason that bulk modulus of ringwoodite is more sensitive to water than shear modulus. *R* of ringwoodite decreases with pressure while *R* of olivine and wadsleyite increases with pressure. *R* reported here was calculated using theoretical method derived equation of states. *R* due to temperature is also reported as a comparison of *R* due to water. The local value of *R* in the upper mantle and transition zone can discriminate between lateral variations of water content and temperature as the origin of lateral seismic variations.

Published by Elsevier B.V.

1. Introduction

The Earth's transition zone has been postulated to be a rich reservoir of water (Bercovici and Karato, 2003, 2004). Wadsleyite and ringwoodite, the high pressure phases of olivine, have a much greater capacity for accommodating H in their crystal structures than does olivine (Smyth, 1994; Smyth et al., 2003). Testing this hypothesis requires defining a metric that is sensitive to water content and insensitive to other variables that are themselves poorly constrained. Seismic velocities provide high resolution observables that reflect on the state of the material. However, radial variations in seismic velocities largely reflect the effects of pressure on the constituent materials, making it difficult to separate out an effect due to water content. Since the sources of water are likely to be spatially variable, concentrated mostly near subduction zones, we would expect that there are large lateral variations in the water content. Here we explore the possibility of detecting lateral variations in water content through lateral variations in seismic velocity. To accomplish this, the effect of water on the seismic velocity must be distinguishable from that of other chemical heterogeneity in chemistry or temperature. We suggest that the correlation of *P* and *S* variations potentially provides such a metric.

The correlation of the variations in *P* and *S* wave velocities, often expressed by the variable, $R = d\ln(Vs)/d\ln(Vs)$, can help identify the specific origin of the underlying heterogeneity. Lateral heterogeneity can be associated with numerous factors, such as temperature, density, chemical composition, water content, attenuation associated with grain size, grain boundary behavior, etc. A particularly interesting feature of *R* is that one can identify individual effects using mineral physics data. For example, we derive $R(H_2O)$ as the ratio between $d\ln(Vs)/d(H_2O)$ and $d\ln(Vp)/d(H_2O)$ and $R(T)$ as the ratio between $d\ln(Vs)/dT$ and $d\ln(Vp)/dT$. By doing so, one can s0eparate and compare the contribution of water and temperature to the lateral heterogeneity.

Studies from *S* and *P* tomographic models (Masters et al., 2000; Robertson and Woodhouse, 1996; Romanowicz, 2001, 2003; Vasco and Johnson, 1998; Vasco et al., 1995) have shown that *R* is a function of depth, with *R* being ~1.7 in the upper mantle, *R* >2.5 in the lower mantle and a maximum of *R* ~3.8 at D''. *R* is also used as a scaling constant in some seismic tomography models (Dueker and Sheehan, 1998). Large *R* indicates that shear wave is affected more than *P* wave by the variable; small *R* indicates that bulk modulus is more sensitive than shear modulus to the variable. In this paper, we will focus on two factors: water content and temperature on iron-free minerals. We focus on the olivine, wadsleyite and ringwoodite which have large capacity for water in the Earth's upper mantle and transition zone (Williams and Hemley, 2001).

2. *R* due to water

There have been a number of papers reporting experimentally measured elasticity of dry and wet olivine (Mao et al., 2010; Zha et al., 1997), wadsleyite (Jacobsen et al., 2009; Mao et al., 2008; Zha et al., 1996) and ringwoodite (Li, 2003; Wang et al., 2003,

---

* Corresponding author.
E-mail address: lilli@ic.sunysb.edu (L. Li).

0031-9201/$ - see front matter Published by Elsevier B.V.
doi:10.1016/j.pepi.2011.07.009

Table 1
Effect of water on Mg_2SiO_4 for olivine α, wadsleyite β and ringwoodite γ at 300 K and 0 GPa from experimental data.

Mg_2SiO_4	$d\rho/dH_2O$	Ks	G	dK/dH_2O	dG/dH_2O	$R(H_2O)$
α (Mao et al., 2010)	0.026	128.8	81.6	3.78	2.22	0.94
β (Mao et al., 2008)	0.046	170.9	111.7	13.8	7.8	1.02
γ (Inoue et al., 1998; Wang et al., 2003)	0.044	184.3	119.5	10.36	5.36	0.76

2006). Table 1 reports $R(H_2O)$ calculated from experimental data at ambient conditions by comparing velocity values of wet and dry samples. Often data from different laboratories are used in the comparison and the total water content of the samples is quite small. Thus, small experimental errors can become magnified in the process of calculating R. Theoretical calculations hold a promise to yield more accurate values of R since the techniques of calculating the properties of both the wet and dry samples are very similar allowing one to focus entirely on the effect of the hydrogen on the acoustic velocities. Elasticity data reported from density functional calculations (Li et al., 2009a; Liu et al., 2009; Panero, 2010; Tsuchiya and Tsuchiya, 2009) is used to derive $R(H_2O)$ for these three phases. These four studies reported elasticity of hydrous Mg_2SiO_4 olivine, wadsleyite and ringwoodite as a function of pressure at zero Kelvin. Water is introduced into olivine structure as defects by either substituting Mg cation or Si cation. Water content ranges from zero percent to saturation (3.3 wt.%) where two Mg atoms are substituted by four hydrogen atoms. To calculate $R(H_2O)$ as a function of pressure, what is needed is the water derivative of elasticity at all pressures, as

$$R = \frac{d\ln Vs}{d\ln Vp} = \frac{d\ln\sqrt{\frac{G}{\rho}}}{d\ln\sqrt{\frac{K+4G/3}{\rho}}} = \left(\frac{G'}{G} - \frac{\rho'}{\rho}\right) \Big/ \left(\frac{K' + \frac{4G'}{3}}{K + \frac{4G}{3}} - \frac{\rho'}{\rho}\right) \qquad (1)$$

where $\rho' = d\rho/d(H_2O)$, $K' = dK/d(H_2O)$, $G' = dG/d(H_2O)$.

Fig. 1 illustrates $R(H_2O)$ as a function of pressure for Mg_2SiO_4 olivine, wadsleyite and ringwoodite. Both experimental and theoretical elasticity data are included here. $R(H_2O)$ for both olivine and wadsleyite shows positive pressure dependence and values large than 1, while $R(H_2O)$ for ringwoodite decreases with pressure and with a value that is significantly less than 1. The interesting pressure dependence of R is associated with the pressure dependence of elasticity of hydrous phases. As illustrated by (Mao et al., 2010), the cross over of P and S wave velocity occurs at around 3 GPa between dry and wet olivine due to lower modulus but higher pressure derive for wet forsterite. But comparing P and S wave velocities of dry and wet ringwoodite (Li, 2003; Wang et al., 2006), wet ringwoodite has both lower bulk modulus and lower pressure derives of bulk modulus, thus the cross over of P and S waves velocity does not occur. R derived from experimental data at ambient conditions is also plotted. R derived from experimental data is slightly less than 1 and close to the calculated results. In general, the theoretical and experimental values agree to better than 0.2 while the expected uncertainty of the theoretical values is about 0.1 because of the consistency of the method.

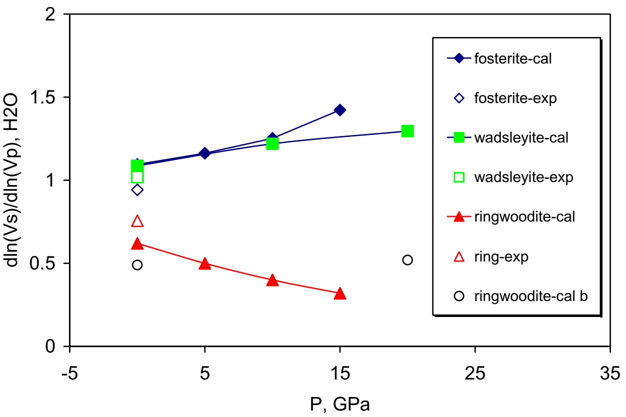

Fig. 1. $R(H_2O)$ for Mg_2SiO_4 olivine, wadsleyite and ringwoodite. Olivine-cal, wadsleyite-cal, ringwoodite-cal are calculated using data from Li et al. (2009a), Liu et al. (2009), Tsuchiya and Tsuchiya (2009)), respectively. Ringwoodite-cal b is taken from Panero (2010). Olivine-exp, wadsleyite-exp, ringwoodite-exp are calculated used data from (Inoue et al. (1998), Li (2003), Mao et al. (2008, 2010), Wang et al. (2003).

3. *R* due to temperature

To calculate $R(T)$ as a function of pressure, one needs the temperature derivative of elasticity as a function of pressure. In Eq. (1), the variables $\rho' = d\rho/dT$, $K' = dK/dT$, $G' = dG/dT$. Experimental data are not measured at mantle pressure–temperature and are thereby limited in deriving $R(T)$ for the pressure–temperature range of the mantle. Furthermore, we wish to maintain consistency in approach with the calculations of $R(H_2O)$. Thus, we use theoretically calculated thermal EOS to provide this information. In a previous paper (Li et al., 2006a), the thermal EOS of ringwoodite has been reported. It uses the *ab inito* molecular dynamics (AIMD) approach, which simulates the stress–strain relation at elevated pressure and temperature conditions, and has been shown to be an accurate method for calculating elastic properties at high pressure and temperature. It explicitly includes temperature in its simulation and has been used successfully to predict the structural and thermo-elastic properties of mantel silicates (Li et al., 2009b, 2006a,b,c; Oganov et al., 2001a,b). Using the resulting thermal EOS, S and P wave velocities can be derived at any mantle pressure and temperature. In this paper, we report the thermal EOS of olivine and wadsleyite using this method. The thermal EOS parameters have been tested that they can successfully predict the available experimental data for olivine and wadsleyite (shown in Figs. 2 and 3). The AIMD symbols in Figs. 2 and 3 are calculated using thermal EOS (listed in Table 2) and extrapolate to the experimental pressure and temperature conditions to compare with the experimental data. Table 3 summarizes the equations of states for olivine, wadsleyite and ringwoodite referenced to the condition of 2000 K and 0 GPa. The formula of calculating the velocities at pressure and temperature can be found in previous papers (Li et al., 2006a; Oganov et al., 2001a) and thus not reported here.

Fig. 4 shows the $R(T)$ for olivine, wadsleyite and ringwoodite at 300 K and 2000 K, respectively. The first point is that pressure has a positive effect on all three minerals. Secondly, $R(T)$ ranges between

Table 2
Thermo-EOS of olivine from AIMD calculations for Mg_2SiO_4 for the reference state of 2000 K and 0 GPa. The EOS of olivine, α and wadsleyite, β are from this study, the EOS of γ is from (Li et al., 2006a).

Mg_2SiO_4	K_T	V_0	K'_T	G	G'	γ_0	q	α_0	δ	dG/dT	dK/dT
α	110.5	613.4	4.15	58.10	2.51	1.10	1.33	3.07 E−05	4.0	−0.007	−0.002
β	147.4	565.0	4.18	82.06	2.60	1.22	1.01	2.88 E−05	4.0	−0.0085	−0.0015
γ	138.0	560	5.2	90.5	2.07	1.34	1.44	3.85 E−05	5.2	−0.0086	0

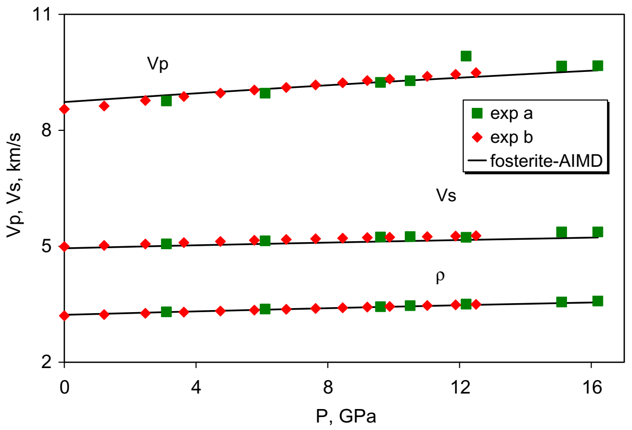

Fig. 2. Comparison between experimental data vs. calculated velocities using thermal EOS of forsterite. Exp a: Zha et al. (1996); Exp b: Li et al. (1996).

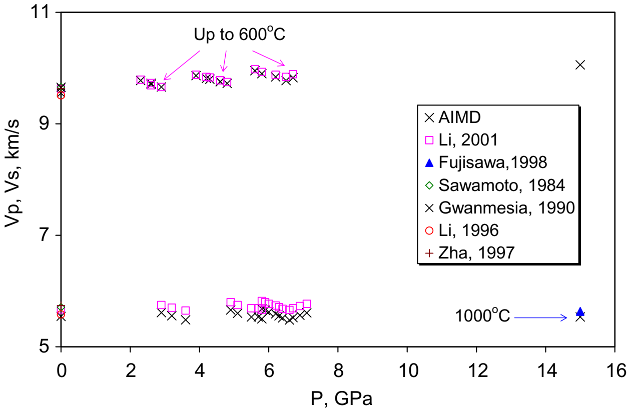

Fig. 3. Comparison between experimental data (Fujisawa, 1998; Gwanmesia et al., 1990; Li, 2003; Li et al., 1996, 2001; Sawamoto et al., 1984; Zha et al., 1997) vs. calculated velocities using thermal EOS of wadsleyite. The experimental data (Li et al., 2001) follows a specific pressure–temperature (P–T) path up to 7 GPa and 600 °C, the AIMD model calculated the velocities at each P–T ultrasonic measurement being made, plus an extra point at 15 GPa and 1000 °C, which was measured by another study (Fujisawa, 1998).

Table 3
$R(T)$ of mantle minerals from experimental data (Jacobsen et al., 2009) at 300 K and 0 GPa.

Mineral	G	K	dG/dT	dK/dT	$R(T)$
Olivine	77	130	−0.014	−0.017	1.23
Wadsleyite	108	173	−0.016	−0.014	1.45
Ringwoodite	119	185	−0.015	−0.019	1.15
1 wt.% H_2O					
Hydrous ol	72	120	−0.013	−0.016	1.21
Hydrous wad	93	155	−0.017	−0.019	1.28
Hydrous ring	105	177	−0.015	−0.021	1.14

1 and 2 for all three minerals, wadsleyite has the highest R value, ringwoodite has the lowest R value. Third, the effect of temperature on R is rather modest in that 300 and 2000 K covers the mantle temperature. The experimental $R(T)$ at ambient conditions is slightly lower than the extrapolated theoretical values (the calculations were all done at higher temperatures).

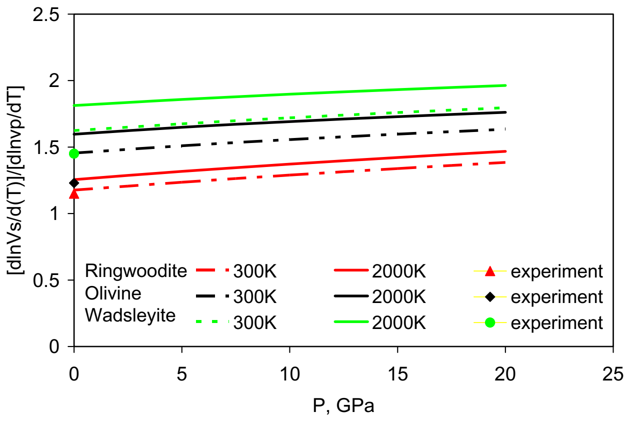

Fig. 4. $R(T)$ of Mg_2SiO_4 olivine, wadsleyite, ringwoodite at 300 K and 2000 K, respectively. Also plotted are laboratory data. Dash lines are at 300 K, solid lines are at 2000 K. Experimental data are listed in Table 3.

4. Summary

This paper demonstrates how water and temperature affect d ln(Vs)/d ln(Vp). Theoretically calculated elasticity parameters are used here to elaborate the pressure dependence on R. Ringwoodite appears to have the lowest of $R(H_2O)$ and $R(T)$ among the three minerals with $R(H_2O)$ being exceedingly low (much less than 1). Furthermore, $R(H_2O)$ of ringwoodite has a negative pressure dependence.

The differences of $R(H_2O)$ and $R(T)$ provide a diagnostic for the origin of lateral variations in seismic velocity for the Earth's upper mantle and transition zone. Fig. 5 illustrates the variation of R with depth for the conditions that lateral seismic variations arise from either lateral variations in temperature or water content. To generate these curves, we assume that the 0 K values of $R(H_2O)$ will be appropriate at mantle temperatures. Lateral variations arising from variations of water content exhibit a much lower value for R throughout this region. The distinction is most pronounced deeper than 500 km where ringwoodite is the dominant phase. Regional determinations of R as a function of depth can thus be used to explore for deep water. Very low values of R (1 or lower) will indicate large lateral variations of water content, while large values (1.5 or greater) will be consistent with lateral variations of temperature.

To date, there have been no reports of low (<1.0) values of R in the transition zone of the Earth. Perhaps, the resolution has not allowed adequate determinations of R for this region. A more compelling conclusion is that R is not small in this region suggesting

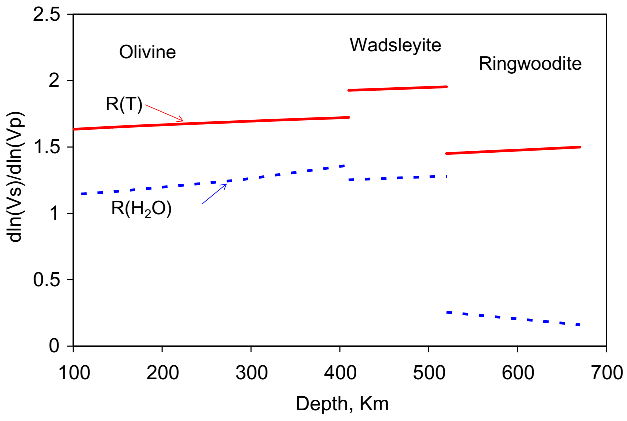

Fig. 5. R as a function of depth for the case of temperature dominated lateral variation in seismic velocity [$R(T)$] or water dominated lateral variation in seismic velocity [$R(H_2O)$]. All values come from density functional theory calculations. The values for $R(H_2O)$ are calculated assuming that there is no temperature dependence of this variable. These curves also assume that the olivine component dominates the value of R in this region.

that lateral water content variations is limited, which further suggests that the total amount of water in this regions is small.

Acknowledgements

This work is support by NERC (Grant Nos. NER/T/S/2001/00855 and NER/O/S/2001/01227), and computer facilities provided by NERC at University College London, and the UK National Supercomputing Service (Hector). The authors acknowledge NSF EAR-9909266, EAR0135551, EAR00135550, EAR1073469 and EAR0809397.

References

Bercovici, D., Karato, S., 2003. Whole-mantle convection and the transition-zone water filter. Nature 425, 39–44.

Bercovici, D., Karato, S., 2004. The transition-zone water-filter model: geochemical implications. Geochim. Cosmochim. Acta 68, A559–A563.

Dueker, K.G., Sheehan, A.F., 1998. Mantle discontinuity structure beneath the Colorado Rocky Mountains and High Plains. J. Geophys. Res. Solid Earth 103, 7153–7169.

Fujisawa, H., 1998. Elastic wave velocities of forsterite and its beta-spinel form and chemical boundary hypothesis for the 410-km discontinuity. J. Geophys. Res. Solid Earth 103, 9591–9608.

Gwanmesia, G.D., Rigden, S.M., Jackson, I., Liebermann, R.C., 1990. Pressure dependence of elastic wave velocity for beta-Mg_2SiO_4 and the composition of the Earth's mantle. Science 250, 794–797.

Inoue, T., Weidner, D.J., Northrup, P.A., Parise, J.B., 1998. Elastic properties of hydrous ringwoodite (gamma-phase) in Mg_2SiO_4. Earth Planet. Sci. Lett. 160, 107–113.

Jacobsen, S.D., Jiang, F.M., Mao, Z., Duffy, T.S., Smyth, J.R., Holl, C.M., Frost, D.J., 2009. Effects of hydration on the elastic properties of olivine (vol. 35, L14303, 2008). Geophys. Res. Lett. 36.

Li, B., 2003. Compressional and shear wave velocities of ringwoodite gamma-Mg_2SiO_4 to 12 GPa. Am. Mineral. 88, 1312–1317.

Li, B., Gwanmesia, G.D., Liebermann, R.C., 1996. Sound velocity of olivine and beta polymorphs of Mg_2SiO_4 at Earth's transition zone pressures. Geophys. Res. Lett. 23, 2259–2262.

Li, B.S., Liebermann, R.C., Weidner, D.J., 2001. P-V-V-p-V-s-T measurements on wadsleyite to 7 GPa and 873 K: implications for the 410-km seismic discontinuity. J. Geophys. Res. Solid Earth 106, 30579–30591.

Li, L., Brodholt, J., Alfè, D., 2009a. Structure and elasticity of hydrous ringwoodite: a first principle investigation. Phys. Earth Planet. Interior 117, 103–115.

Li, L., Weidner, D.J., Brodholt, J., Alfè, D., Price, G.D., 2009b. Ab initio molecular dynamics study of elasticity of akimotoite $MgSiO_3$ at mantle conditions. Phys. Earth Planet. Interior 173, 115–120.

Li, L., Weidner, D.J., Brodholt, J., Alfè, D., Price, G.D., 2006a. Elasticity of Mg_2SiO_4 ringwoodite at mantle conditions. Phys. Earth Planet. Interior 157, 181–187.

Li, L., Weidner, D.J., Brodholt, J., Alfè, D., Price, G.D., Caraca, R., Wentzcovitch, R., 2006b. Elasticity of $CaSiO_3$ perovskite at high pressure and high temperature. Phys. Earth Planet. Sci. 155, 249–259.

Li, L., Weidner, D.J., Brodholt, J., Alfè, D., Price, G.D., Caracas, R., Wentzcovitch, R., 2006c. Phase stability of $CaSiO_3$ perovskite at high pressure and temperature: insights from ab initio molecular dynamics. Phys. Earth Planet. Sci. 155, 260–268.

Liu, L., Du, J.G., Zhao, J.J., Liu, H., Gao, H.L., Chen, Y.X., 2009. Elastic properties of hydrous forsterites under high pressure: first-principle calculations. Phys. Earth Planet. Interior 176, 89–97.

Mao, Z., Jacobsen, S.D., Jiang, F., Smyth, J.R., Holl, C.M., Duffy, T.S., 2008. Elasticity of hydrous wadsleyite to 12 GPa: implications for Earth's transition zone. Geophys. Res. Lett., 1–5.

Mao, Z., Jacobsen, S.D., Jiang, F., Smyth, J.R., Holl, C.M., Frost, D.J., Duffy, T.S., 2010. Velocity crossover between hydrous and anhydrous forsterite at high pressures. Earth Planet. Sci. Lett. 293, 250–258.

Masters, G., Laske, G., Bolton, H., Dziewonski, A.M., 2000. The relative behavior of shear velocity, bulk sound speed, and compressional velocity in the mantle: implications for chemical and thermal structure. In: Karato, S.-i., Fortes, A.D., Lieberman, R.C., Masters, G., Stixrude, L. (Eds.), Earth's Deep Interior: Mineral Physics and Tomography from the Atomic to the Global Scale. AGU, Washington, DC, pp. 63–87.

Oganov, A.R., Brodholt, J.P., Price, G.D., 2001a. Ab initio elasticity and thermal equation of state of $MgSiO_3$ perovskite. Earth Planet. Sci. Lett. 184, 555–560.

Oganov, A.R., Brodholt, J.P., Price, G.D., 2001b. The elastic constants of $MgSiO_3$ perovskite at pressures and temperatures of the Earth's mantle. Nature (London) 411, 934–937.

Panero, W.R., 2010. First principles determination of the structure and elasticity of hydrous ringwoodite. J. Geophys. Res. Solid Earth, 1–11.

Robertson, G.S., Woodhouse, J.H., 1996. Constraints on lower mantle physical properties from seismology and mineral physics. Earth Planet. Sci. Lett. 143, 197–205.

Romanowicz, B., 2001. Can we resolve 3D density heterogeneity in the lower mantle? Geophys. Res. Lett. 28, 1107–1110.

Romanowicz, B., 2003. Global mantle tomography: progress status in the past 10 years. Annu. Rev. Earth Planet. Sci. 31, 303–328.

Sawamoto, H., Weidner, D.J., Sasaki, S., Kumazawa, M., 1984. Singlecrystal elastic properties of the modified-spinel (beta) phase of magnesium orthosilicate. Science 224, 749–751.

Smyth, J.R., 1994. A crystallographic model for hydrous wadsleyite (beta-Mg_2SiO_4) – an ocean in the Earths interior. Am. Mineral. 79, 1021–1024.

Smyth, J.R., Holl, C.M., Frost, D.J., Jacobsen, S.D., Langenhorst, F., McCammon, C.A., 2003. Structural systematics of hydrous ringwoodite and water in Earth's interior. Am. Mineral. 88, 1402–1407.

Tsuchiya, J., Tsuchiya, T., 2009. First principles investigation of the structural and elastic properties of hydrous wadsleyite under pressure. J. Geophys. Res. Solid Earth, 1–13.

Vasco, D.W., Johnson, L.R., 1998. Whole earth structure estimated from seismic arrival times. J. Geophys. Res. Solid Earth 103, 2633–2671.

Vasco, D.W., Johnson, L.R., Pulliam, J., 1995. Lateral variations in mantle velocity structure and discontinuities determined from P, PP, S, SS, and SS-SdS travel time residuals. J. Geophys. Res. Solid Earth 100, 24037–24059.

Wang, J.Y., Sinogeikin, S.V., Inoue, T., Bass, J.D., 2003. Elastic properties of hydrous ringwoodite. Am. Mineral. 88, 1608–1611.

Wang, J.Y., Sinogeikin, S.V., Inoue, T., Bass, J.D., 2006. Elastic properties of hydrous ringwoodite at high-pressure conditions. Geophys. Res. Lett., 1–4.

Williams, Q., Hemley, R.J., 2001. Hydrogen in the deep earth. Annu. Rev. Earth Planet. Sci. 29, 365–418.

Zha, C.S., Duffy, T.S., Downs, R.T., Mao, H.K., Hemley, R.J., 1996. Sound velocity and elasticity of single-crystal forsterite to 16 GPa. J. Geophys. Res. Solid Earth 101, 17535–17545.

Zha, C.S., Duffy, T.S., Mao, H.K., Downs, R.T., Hemley, R.J., Weidner, D.J., 1997. Single-crystal elasticity of beta-Mg_2SiO_4 to the pressure of the 410 km seismic discontinuity in the Earth's mantle. Earth Planet. Sci. Lett. 147, E9–E15.